

This article is published as part of the *Dalton Transactions* themed issue entitled:

Molecular Magnets

Guest Editor Euan Brechin
University of Edinburgh, UK

Published in [issue 20, 2010](#) of *Dalton Transactions*

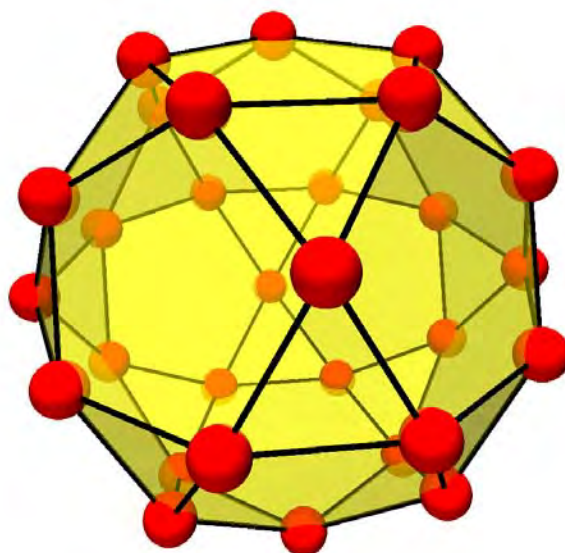


Image reproduced with permission of Jürgen Schnack

Articles in the issue include:

PERSPECTIVES:

[Magnetic quantum tunneling: insights from simple molecule-based magnets](#)

Stephen Hill, Saiti Datta, Junjie Liu, Ross Inglis, Constantinos J. Milios, Patrick L. Feng, John J. Henderson, Enrique del Barco, Euan K. Brechin and David N. Hendrickson, *Dalton Trans.*, 2010, DOI: 10.1039/c002750b

[Effects of frustration on magnetic molecules: a survey from Olivier Kahn until today](#)

Jürgen Schnack, *Dalton Trans.*, 2010, DOI: 10.1039/b925358k

COMMUNICATIONS:

[Pressure effect on the three-dimensional charge-transfer ferromagnet \[Ru₂\(m-FPhCO₂\)₄\]₂\(BTDA-TCNQ\)\]](#)

Natsuko Motokawa, Hitoshi Miyasaka and Masahiro Yamashita, *Dalton Trans.*, 2010, DOI: 10.1039/b925685g

[Slow magnetic relaxation in a 3D network of cobalt\(II\) citrate cubanes](#)

Kyle W. Galloway, Marc Schmidtman, Javier Sanchez-Benitez, Konstantin V. Kamenev, Wolfgang Wernsdorfer and Mark Murrie, *Dalton Trans.*, 2010, DOI: 10.1039/b924803j

Visit the *Dalton Transactions* website for more cutting-edge inorganic and organometallic research
www.rsc.org/dalton

Ferromagnetically coupled chiral cyanide-bridged $\{\text{Ni}_6\text{Fe}_4\}$ cages†

Takuya Shiga,^a Graham N. Newton,^a Jennifer S. Mathieson,^b Tamaki Tetsuka,^a Masayuki Nihei,^a Leroy Cronin^b and Hiroki Oshio^{*a}

Received 2nd December 2009, Accepted 8th January 2010

First published as an Advance Article on the web 21st January 2010

DOI: 10.1039/b925399h

Enantiomeric, ferromagnetically coupled decanuclear $\{\text{Ni}_6\text{Fe}_4\}$ cages with adamantane-like cores were synthesized around templating tetraethylammonium cations, as shown by crystallographic analysis and CSI-MS, and their homochiral nature was confirmed by circular dichroism measurements.

In recent years functional molecules have helped to underpin dramatic developments in the field of nano-scale materials. Nano-capsules are a class of molecular materials in which the functionality can be precisely defined (especially in the case of supramolecular inclusion complexes/sensors), as it is possible to engineer specific spaces for reactions to occur, under the dynamic conditions associated with host/guest systems.¹⁻⁴ Polynuclear transition metal complexes are interesting potential candidates to form cage compounds as the cage itself may be endowed with a large spin ground state and negative magnetic anisotropy resulting in quantum magnetism that could give rise to physical phenomena.⁵ It goes without saying that design plays a critical role in the development of these clusters, particularly as we are now gaining an understanding of how precise control of magnetic properties can be achieved through subtle alterations in the ligand structure.⁶ The introduction of chirality into a system can result in interesting optical and magneto-optical properties as well as ferroelectricity, as a result of the asymmetric dipole moment.^{7,8} Further, in the field of chiral magnetism, unique properties such as magneto-chiral dichroism have been reported,⁹ and the synergy between multiple physical properties may be the key to developing novel functionality.¹⁰ To date, we have reported large (nano-scale) molecular-based magnetic systems, and their quantum properties and multi-stabilities have been discussed.¹¹ In order to combine the physical properties derived from the introduction of ligands that allow chiral complexes and cages to form, with molecular magnetism, we must focus on the rational synthesis of chiral complexes with high spin ground states, where all metal centers have the same absolute configuration with respect to their coordination environment. Herein, we report the syntheses, structures and magnetic properties of two ferromagnetically coupled decanuclear

complexes with chiral cage structures, obtained in the course of synthesising functional materials which exhibit both magnetic properties and chirality.

The reaction of 2-pyridine carbaldehyde, *R*-phenyl ethyl amine and nickel chloride hexahydrate in a 2:2:1 ratio in methanol gives rise to the chiral nickel precursor complex $[\text{Ni}(\text{L}^{\text{R}})_2\text{Cl}_2]$ (**1R**, $\text{L}^{\text{R}} = N$ -(2-pyridylmethylene)-(*R*)-1-phenylethylamine) and the chiral $\{\text{Ni}_6\text{Fe}_4\}$ decanuclear complex, $(\text{Et}_4\text{N})[\text{Ni}(\text{L}^{\text{R}})_6][\text{Fe}(\text{CN})_6]_4(\text{PF}_6)_2 \cdot 22\text{H}_2\text{O} \cdot 26\text{CH}_3\text{OH}$ (**2R**) was obtained by the reaction of **1R** with $(\text{Et}_4\text{N})_3[\text{Fe}(\text{CN})_6]$ and NH_4PF_6 in $\text{MeOH}-\text{H}_2\text{O}$. The corresponding enantiomers **1S** and **2S** were prepared by the same method using L^{S} ($\text{L}^{\text{S}} = N$ -(2-pyridylmethylene)-(*S*)-1-phenylethylamine) in place of L^{R} .

The structure of **1R**, which was obtained by recrystallization, contains a dinuclear unit and a mononuclear unit, and can be described as $[\text{Ni}_2\text{Cl}_2(\text{L}^{\text{R}})_4][\text{NiCl}_2(\text{L}^{\text{R}})_2]\text{Cl}_2 \cdot 3\text{MeOH}$ (Fig. S1†). Each nickel ion adopts an octahedral coordination environment, coordinated by four nitrogen atoms from two bidentate L^{R} ligands and two chloride ions. There are $\pi-\pi$ stacking interactions between the pyridyl and phenyl rings of the two chiral ligands. Consequently, all nickel ions have Λ -type coordination geometry. Likewise, when L^{S} was used, a homo chiral **1S** complex with Δ -type configuration was obtained. Both **1R** and **1S** crystallized in the chiral space group, *P1*, as confirmed by the Flack parameters; 0.009(8) for **1R** and 0.000(11) for **1S**, respectively.

The structure of the chiral decanuclear $\{\text{Ni}_6\text{Fe}_4\}$ cage **2R** derived from the homochiral precursor **1R** is shown in Fig. 1. Four nitrogen atoms from two ligand molecules and the nitrogen atoms from two cyano groups coordinate to the nickel ions, resulting in octahedral coordination environments. The $[\text{Ni}(\text{L}^{\text{R}})_2]$ units are connected to the $[\text{Fe}(\text{CN})_6]^{3-}$ units via the nitrogen atoms of *fac*- CN^- ligands, so that each nickel center is associated with two iron ions, and each iron center has bridges to three nickels. **2R** consists of six $[\text{Ni}(\text{L}^{\text{R}})_2]^{2+}$ and four $[\text{Fe}(\text{CN})_6]^{3-}$ units to form a neutral decanuclear cyanide-bridged cage with an adamantane-like metal arrangement. It is worthy to note that the adamantane-like motif is a new variation among reported discrete cyanide-bridged clusters.¹² All six nickel ions exhibit identical Λ -type absolute configuration as in **1R** due to the $\pi-\pi$ stacking between neighboring ligands. One tetraethylammonium cation is captured by the cage as a template and one hexafluorophosphate ion exists in the lattice as a counter anion. The intracluster separations between nickel and iron ions range from 5.030 to 5.070 Å, and the shortest metal-metal intermolecular distance is 10.454 Å between Ni ions. When using the homochiral enantiomer nickel complex **1S**, the corresponding homochiral **2S** decanuclear complex with Δ -type nickel configuration was formed (Fig. S2†). These absolute structures were confirmed on the basis of the Flack parameters;

^aDepartment of Chemistry, Graduate School of Pure and Applied Sciences, University of Tsukuba, Tennodai 1-1-1, Tsukuba, 305-8571, Japan. E-mail: oshio@chem.tsukuba.ac.jp; Fax: +81 29 853 4238; Tel: +81 29 853 4238

^bWestCHEM, Department of Chemistry, The University of Glasgow, University Avenue, Glasgow, G12 8QQ, UK. E-mail: L. Cronin@chem.gla.ac.uk; Fax: +44-141-330-4888; Tel: +44-141-330-6650

† Electronic supplementary information (ESI) available: Additional figures and experimental procedures. CCDC reference numbers 756354, 756355, 756356, 756357 for **1R**, **1S**, **2R**, **2S** respectively. For ESI and crystallographic data in CIF or other electronic format see DOI: 10.1039/b925399h

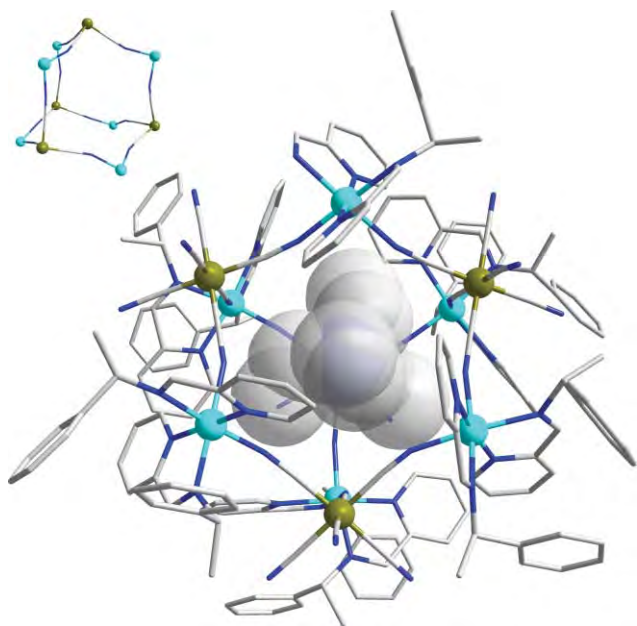


Fig. 1 Molecular structure of **2R**. Colour code: C grey, N light blue, Ni green, Fe brown. Inset: the adamantane-like core.

0.09(2) for **2R** and 0.057(17) for **2S**. The structural incarceration of the templating tetraethylammonium cation is confirmed by CSI-MS measurements carried out at $-20\text{ }^{\circ}\text{C}$, which show that the cage exists as a dication in solution with the formula $[(\text{Et}_4\text{N})\text{X}[\text{Ni}(\text{L}^{\text{S}})_2]_6[\text{Fe}(\text{CN})_6]_4]^{2+}$ for both homochiral species **2R** and **2S**, where $\text{X} = \text{H}, \text{Na}, \text{K}$ (Fig. 2 and S3†).¹³

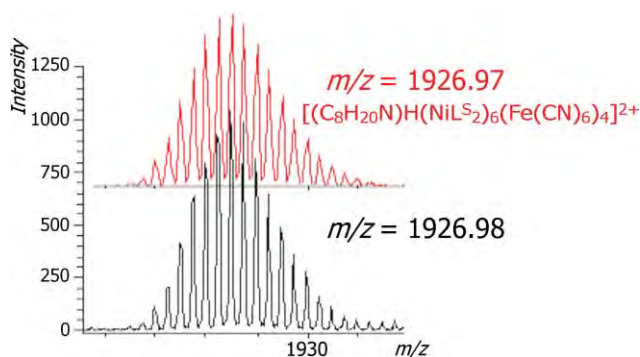


Fig. 2 CSI-MS spectra of **2S**, showing the primary cluster peak observed (black) and the assignment (red).

Similar synthetic methods have been used to generate numerous cyanide-bridged networks using bidentate diamine ligands.¹⁴ For example, two-dimensional bimetallic networks $[\text{Ni}(\text{diamine})_2]_2[\text{Fe}(\text{CN})_6]\text{X}$ (diamine = 1,2-propanediamine or 1,1-dimethylethylenediamine, $\text{X} = \text{Cl}^-, \text{ClO}_4^-, \text{PF}_6^-$), were synthesized by almost the same synthetic method as the present compounds with the exception of the ligand and the base used. It is suggested that the chiral bidentate ligands L^{S} and L^{R} stabilize a *cis*-form mononuclear intermediate in solution due to their π - π stacking in the synthesis of **2R** and **2S**, thus disfavoring the formation of extended network structures.

Magnetic susceptibility measurements for a powdered sample of **2R** were performed in the temperature range of 1.8–300 K. The $\chi_{\text{m}}T$ value at 300 K is $9.84\text{ emu mol}^{-1}\text{ K}$, which is larger than the value expected for six uncorrelated Ni(II) ions and four low-spin Fe(III) ions ($7.5\text{ emu mol}^{-1}\text{ K}$, $g = 2.00$). The $\chi_{\text{m}}T$ values gradually increased as the temperature was lowered, reaching a maximum value of $34.81\text{ emu mol}^{-1}\text{ K}$ at 2.2 K. This behaviour is an indication that the magnetic interactions between the metal ions are ferromagnetic, as expected due to the orthogonality of the e_{g} magnetic orbitals of the Ni(II) ions and the $t_{2\text{g}}$ magnetic orbitals of the low-spin Fe(III) ions. The Curie–Weiss plot gave a positive Weiss constant ($C = 9.67\text{ emu mol}^{-1}\text{ K}$ and $\theta = +5.11\text{ K}$ in the range of 50–300 K), which suggested relatively strong ferromagnetic interactions in operation between metal ions. Plots of the magnetization data at 1.8 K as a function of the applied magnetic field up to 5 T are shown in Fig. 3 (inset). The $M/N\beta$ values increased with increasing magnetic field strength, and did not show saturation up to 5 T, which corresponds to the existence of zero-field splitting due to the low structural symmetry derived from the adamantane-like metal arrangement. The value of magnetization at 5 T is close to the expected value for $S_{\text{T}} = 8$. To examine the nature of the ground states and zero-field splitting, variable field magnetization measurements were carried out in 1–5 T fields in the range of 1.8–4.0 K (Fig. S4†). The non-superposability of the isolated lines confirms the existence of significant zero-field splitting due to the molecular structure having a pseudo tetrahedral symmetry. The reduced magnetization data in the 1.8–2.4 K and 2–5 T ranges were fitted assuming a $S_{\text{T}} = 8$ ground state with $g = 2.00$ and $D/k_{\text{B}} = -0.28\text{ K}$ for **2R**. The Δ -type enantiomer **2S** shows similar ferromagnetic interactions (Fig. S5, S6†), which are confirmed by the positive Weiss constant ($C = 10.04\text{ emu mol}^{-1}\text{ K}$ and $\theta = +4.54\text{ K}$ in the range of 50–300 K) and the magnetization behaviour (reduced magnetization data were fitted with $S_{\text{T}} = 8$, $g = 2.00$ and $D/k_{\text{B}} = -0.29\text{ K}$). To confirm the sign and magnitude of the D value, high-field EPR measurements at low temperature will be required.

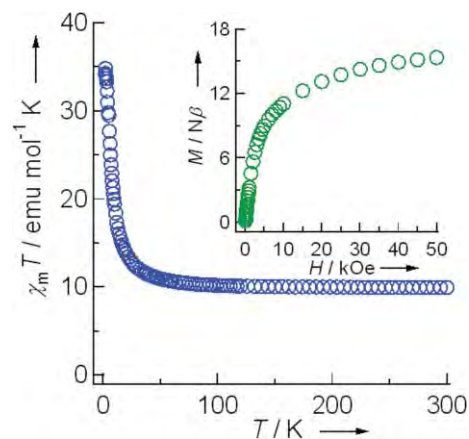


Fig. 3 Plot of $\chi_{\text{m}}T$ vs. T of **2R** at an applied field of 500 Oe. Inset: Field dependence of the magnetization at 1.8 K.

UV-vis spectra in acetonitrile for both **2R** and **2S** were collected, showing absorption peaks at 900 nm and 415 nm, which were assigned to the d–d transitions of Ni(II) ions and charge transfer from cyanide to Fe(III) centers, respectively (Fig. S7†). Circular

dichroism measurements for **2R** and **2S** were performed in acetonitrile and KCl pellets (Fig. 4 and S8†). Well-defined peaks confirm the enantiomeric nature of these complexes. **2R** and **2S** gave mirror-symmetrical CD spectra, providing evidence of the homochiral nature of both.

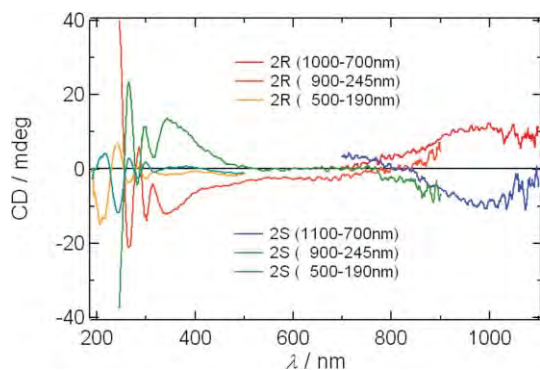


Fig. 4 CD data obtained from a transparent disk with a radius of 5 mm made from a mixture of crystalline **2R** (or **2S**) and KCl (see ESI†).

In conclusion, we have obtained novel homochiral decanuclear nickel-iron cyanide bridged complexes with an $S_T = 8$ ground state due to ferromagnetic interactions between nickel and iron ions. The homochiral nature of the structures was confirmed crystallographically by the Flack parameters and through CD spectrometry. Various combinations of other transition metal ions and polycyanometallates with chiral ligands, which can induce absolute structures, may lead to multifunctional nanoclusters displaying both chirality and interesting magnetic properties. Moreover, specific cage structures may lead to selective-recognition of chiral molecules and the magnetic field effect on the host/guest complexes will be investigated.

$[\text{NiCl}_2(\text{L}^R)_2]$ (**1R**): $\text{NiCl}_2 \cdot 6\text{H}_2\text{O}$ (3.56 g, 15 mmol) in methanol (25 ml) was added to 2-pyridine carbaldehyde (3.21 g, 30 mmol) and *R*-phenyl ethyl amine (3.64 g, 30 mmol) in methanol (50 ml). The resulting light green solution was allowed to evaporate and crystalline green solid $[\text{NiCl}_2(\text{L}^R)_2]$ (**1R**) formed. Yield 8.434 g (92%). Since the resulting green precipitate was deliquescent, the dried precipitate was used for the following syntheses of **2R**. Light-green square plates were recrystallized from methanol by ether diffusion. Anal. calcd. (found) for $(\text{C}_{84}\text{H}_{104}\text{N}_{12}\text{Cl}_6\text{Ni}_3\text{O}_{10})$: C, 55.11 (55.36); H, 5.73 (5.71); N, 9.18 (9.10).

$[\text{NiCl}_2(\text{L}^S)_2]$ (**1S**): **1S** was obtained by the same synthetic approach as **1R** with L^S in place of L^R . Yield 8.711 g (92%). Anal. calcd. (found) for $(\text{C}_{84}\text{H}_{110}\text{Cl}_6\text{N}_{12}\text{Ni}_3\text{O}_{13})$: C, 53.53 (53.34); H, 5.88 (5.76); N, 8.92 (8.90).

$(\text{Et}_4\text{N})[\text{Ni}(\text{L}^R)_2]_6[\text{Fe}(\text{CN})_6]_4(\text{PF}_6)_2 \cdot 22\text{H}_2\text{O} \cdot 26\text{CH}_3\text{OH}$ (**2R**): A methanol– H_2O mixed solution (20 ml) of **1R** (55 mg) and NH_4PF_6 (64 mg, 0.4 mmol) was diffused to $(\text{Et}_4\text{N})_3[\text{Fe}(\text{CN})_6]$ (60 mg, 0.1 mmol) in methanol (20 ml) at 5 °C and light-brown hexagonal plates of $(\text{Et}_4\text{N})[\text{Ni}(\text{L}^R)_2]_6[\text{Fe}(\text{CN})_6]_4(\text{PF}_6)_2 \cdot 22\text{H}_2\text{O}$ (**2R**) were obtained. Yield ca. 90%. Anal. calcd. (found) for $\text{C}_{200}\text{H}_{176}\text{N}_{49}\text{F}_6\text{P}_1\text{Fe}_4\text{Ni}_6 \cdot 22(\text{H}_2\text{O})$: C, 54.81 (54.18); H, 5.06 (5.10); N, 15.66 (15.85).

$(\text{Et}_4\text{N})[\text{Ni}(\text{L}^S)_2]_6[\text{Fe}(\text{CN})_6]_4(\text{PF}_6)_2 \cdot 22\text{H}_2\text{O} \cdot 28\text{CH}_3\text{OH}$ (**2S**): Obtained by the same synthetic approach as **2R**, but using **1S** instead of **1R**. Yield ca. 90%. Anal. calcd. (found) for

$\text{C}_{200}\text{H}_{176}\text{N}_{49}\text{F}_6\text{P}_1\text{Fe}_4\text{Ni}_6 \cdot 22(\text{H}_2\text{O})$: C, 54.81 (54.54); H, 5.06 (5.01); N, 15.66 (16.02).

X-ray structural analysis of **1R**: light-green square plates, $0.40 \times 0.40 \times 0.32 \text{ mm}^3$, $\text{C}_{87}\text{H}_{96}\text{N}_{12}\text{Cl}_6\text{Ni}_3\text{O}_3$, $M = 1746.53$, triclinic, $P1$ (No.1), $T = 200 \text{ K}$, $a = 10.3057(17)$, $b = 14.806(2)$, $c = 15.877(3)$, $\alpha = 107.701(2)$, $\beta = 107.261(2)$, $\gamma = 99.251(2)$, $V = 2118.6(6) \text{ \AA}^3$, $Z = 1$, $\rho_c = 1.369 \text{ gm}^{-3}$, final $R_1 = 0.0273$ ($I > 2\sigma(I)$), $wR_2 = 0.0721$ (all data), GOF = 1.024, Flack parameter = 0.009(8). Non-H atoms were refined anisotropically for all data sets. H atoms were added with ideal geometry.

X-ray structural analysis of **1S**: light-green square plates, $0.50 \times 0.20 \times 0.18 \text{ mm}^3$, $\text{C}_{87}\text{H}_{96}\text{N}_{12}\text{Cl}_6\text{Ni}_3\text{O}_3$, $M = 1746.53$, triclinic, $P1$ (No.1), $T = 200 \text{ K}$, $a = 10.3220(17)$, $b = 14.819(3)$, $c = 15.883(3)$, $\alpha = 107.650(3)$, $\beta = 107.289(2)$, $\gamma = 99.278(3)$, $V = 2124.6(6) \text{ \AA}^3$, $Z = 1$, $\rho_c = 1.365 \text{ gm}^{-3}$, final $R_1 = 0.0385$ ($I > 2\sigma(I)$), $wR_2 = 0.0908$ (all data), GOF = 1.001, Flack parameter = 0.000(11).

X-ray structural analysis of **2R**: brown hexagonal plates, $0.50 \times 0.50 \times 0.05 \text{ mm}^3$, $\text{C}_{233}\text{H}_{332}\text{F}_4\text{Fe}_4\text{Ni}_6\text{O}_{41}\text{P}_6$, $M = 4362.48$, trigonal, $P3$ (No.143), $T = 200 \text{ K}$, $a = 19.567(5)$, $c = 35.123(13)$, $V = 11646(6) \text{ \AA}^3$, $Z = 2$, $\rho_c = 1.460 \text{ gm}^{-3}$, final $R_1 = 0.0811$ ($I > 2\sigma(I)$), $wR_2 = 0.1979$ (all data), GOF = 0.875, Flack parameter = 0.09(2). The *hkl* file was processed with SQUEEZE to eliminate disordered solvent molecules for **2R** and **2S**.

X-ray structural analysis of **2S**: brown hexagonal plates, $0.50 \times 0.50 \times 0.05 \text{ mm}^3$, $\text{C}_{233}\text{H}_{340}\text{F}_6\text{Fe}_4\text{Ni}_6\text{O}_{43}\text{P}$, $M = 5236.17$, trigonal, $P3$ (No.143), $T = 200 \text{ K}$, $a = 19.574(3)$, $c = 35.075(9)$, $V = 11638(4) \text{ \AA}^3$, $Z = 2$, $\rho_c = 1.494 \text{ gm}^{-3}$, final $R_1 = 0.0684$ ($I > 2\sigma(I)$), $wR_2 = 0.1556$ (all data), GOF = 0.780, Flack parameter = 0.057(17).

Notes and references

- (a) D. Fiedler, D. H. Leung, R. G. Bergman and K. N. Raymond, *Acc. Chem. Res.*, 2005, **38**, 349; (b) M. D. Pluth and K. N. Raymond, *Chem. Soc. Rev.*, 2007, **36**, 161; (c) M. D. Pluth, R. G. Bergman and K. N. Raymond, *Science*, 2007, **316**, 85.
- (a) S. Leininger, B. Olenyuk and P. J. Stang, *Chem. Rev.*, 2000, **100**, 853; (b) S. R. Seidel and P. J. Stang, *Acc. Chem. Res.*, 2002, **35**, 972; (c) Q.-H. Yuan, L.-J. Wan, H. Jude and P. J. Stang, *J. Am. Chem. Soc.*, 2005, **127**, 16279.
- (a) M. Yoshizawa, M. Tamura and M. Fujita, *Science*, 2006, **312**, 251; (b) M. Fujita, M. Tominaga, A. Hori and B. Therrien, *Acc. Chem. Res.*, 2005, **38**, 369.
- (a) L. Cronin, *Angew. Chem., Int. Ed.*, 2006, **45**, 3576; (b) K. Harano, S. Hiraoka and M. Shionoya, *J. Am. Chem. Soc.*, 2007, **129**, 5300.
- (a) D. Gatteschi and R. Sessoli, *Angew. Chem., Int. Ed.*, 2003, **42**, 268; (b) D. Gatteschi, R. Sessoli, and J. Villain, "Molecular Nanomagnets", 2006, Oxford University Press.
- R. Inglis, L. F. Jones, C. J. Milios, S. Datta, A. Collins, S. Parsons, W. Wernsdorfer, S. Hill, S. P. Perlepes, S. Piligkos and E. K. Brechin, *Dalton Trans.*, 2009, 3403.
- I. W. Samuel, J. Zyss, M. Bourgault and H. L. Bozec, *Nature*, 1995, **374**, 339.
- (a) Q. Ye, Y.-M. Song, G.-X. Wang, K. Chen, D.-W. Fu, P. W. H. Chan, J.-S. Zhu, S.D. Huang and R.-G. Xiong, *J. Am. Chem. Soc.*, 2006, **128**, 6554; (b) S. V. Yablonskii, E. A. Soto-Bustanante, R. O. Vergara-Tolosa and W. Haase, *Adv. Mater.*, 2004, **16**, 1936; (c) T. Kimura, T. Goto, H. Shintani, K. Ishizaka, T. Arima and Y. Tokura, *Nature*, 2003, **426**, 55.
- G. L. J. Rikken and E. Raupach, *Nature*, 1997, **390**, 493.
- (a) K. Inoue, K. Kikuchi, M. Ohba and H. Ōkawa, *Angew. Chem., Int. Ed.*, 2003, **42**, 4810; (b) H. Imai, K. Inoue, K. Kikuchi, Y. Yoshida, M. Ito, T. Sunahara and S. Onaka, *Angew. Chem., Int. Ed.*, 2004, **43**(42), 5618; (c) E. Coronado, C. J. Gómez-García, A. Nuez, F. M. Romero and J. C. Waerenborgh, *Chem. Mater.*, 2006, **18**, 2670; (d) W. Kaneko, S. Kitagawa and M. Ohba, *J. Am. Chem. Soc.*, 2007, **129**, 248; (e) S. Decurtins, H. W. Schmalke, P. Seneuwly and H. R. Oswald,

- Inorg. Chem.*, 1993, **32**, 1888; (f) E. Coronado, J. R. Galán-Mascarós, C. J. Gómez-García and J. M. Martínez-Agudo, *Inorg. Chem.*, 2001, **40**, 113.
- 11 (a) H. Oshio, N. Hoshino, T. Ito and M. Nakano, *J. Am. Chem. Soc.*, 2004, **126**, 8805; (b) H. Oshio, N. Hoshino and T. Ito, *J. Am. Chem. Soc.*, 2000, **122**, 12602; (c) M. Nihei, M. Ui, M. Yokota, L. Han, A. Maeda, H. Kishida, H. Okamoto and H. Oshio, *Angew. Chem., Int. Ed.*, 2005, **44**, 6484.
- 12 (a) D. Li, R. Clérac, O. Roubeau, E. Harté, C. Mathonière, R. L. Bris and S. M. Holmes, *J. Am. Chem. Soc.*, 2008, **130**, 252; (b) J. M. Herrera, V. Marvaud, M. Verdaguer, J. Marrot, M. Kalisz and C. Mathonière, *Angew. Chem., Int. Ed.*, 2004, **43**, 5468; (c) J. L. Heinrich, P. A. Berseth and J. R. Long, *Chem. Commun.*, 1998, 1231; (d) T. D. Harris and J. R. Long, *Chem. Commun.*, 2007, 1360; (e) M. Shatruk, A. Dragulescu-Andrasi, K. E. Chambers, S. A. Stoian, E. L. Bominaar, C. Achim and K. R. Dunbar, *J. Am. Chem. Soc.*, 2007, **129**, 6104.
- 13 (a) H. N. Miras, E. F. Wilson and L. Cronin, *Chem. Commun.*, 2009, 1297; (b) G. J. T. Cooper, G. N. Newton, D.-L. Long, P. Kögerler, M. H. Rosnes, M. Keller and L. Cronin, *Inorg. Chem.*, 2009, **48**, 1097; (c) G. N. Newton, G. J. T. Cooper, P. Kögerler, D. L. Long and L. Cronin, *J. Am. Chem. Soc.*, 2008, **130**, 790.
- 14 (a) M. Ohba, H. Ōkawa, N. Fukita and Y. Hashimoto, *J. Am. Chem. Soc.*, 1997, **119**, 1011; (b) M. Ohba and H. Ōkawa, *Coord. Chem. Rev.*, 2000, **198**, 313.